

Traj-Explainer: An Explainable and Robust Multi-modal Trajectory Prediction Approach

Pei Liu¹, Haipeng Liu², Yiqun Li³, Tianyu Shi⁴, Meixin Zhu¹, Ziyuan Pu^{3*}

¹Intelligent Transportation Thrust, Systems Hub, The Hong Kong University of Science and Technology (Guangzhou), Guangzhou, 511458, China

²Li Auto Inc, Jiading District, Shanghai, 201800, China

³School of Transportation, Southeast University, Nanjing, 211189, China

⁴Department of Computer Science, University of Toronto, Toronto, Canada

Abstract

Navigating complex traffic environments has been significantly enhanced by advancements in intelligent technologies, enabling accurate environment perception and trajectory prediction for automated vehicles. However, existing research often neglects the consideration of the joint reasoning of scenario agents and lacks interpretability in trajectory prediction models, thereby limiting their practical application in real-world scenarios. To this purpose, an explainability-oriented trajectory prediction model is designed in this work, named Explainable Conditional Diffusion based Multimodal Trajectory Prediction (Traj-Explainer), to retrieve the influencing factors of prediction and help understand the intrinsic mechanism of prediction. In Traj-Explainer, a modified conditional diffusion is well designed to capture the scenario multimodal trajectory pattern, and meanwhile, a modified Shapley Value model is assembled to rationally learn the importance of the global and scenario features. Numerical experiments are carried out by several trajectory prediction datasets, including Waymo, NGSIM, HighD, and MoCAD datasets. Furthermore, we evaluate the identified input factors which indicates that they are in agreement with the human driving experience, indicating the capability of the proposed model in appropriately learning the prediction. Code available in our open-source repository: <https://anonymous.4open.science/r/Interpretable-Prediction>.

Introduction

Motion prediction, in the autonomous driving setting, refers to predicting the future trajectories of the target agents with the considerations of the historical and current status of the target agents, context agents, road graphs, and traffic light signals, which still contain several challenges for guaranteeing the safe navigation of autonomous vehicles under various environmental uncertainties. (Feng et al. 2023; Zhou et al. 2023) First of all, motion prediction requires the joint reasoning of the future distributions of the surrounding agents that may interact with each other. Naively predicting and sampling from the marginal distribution of trajectories for each agent leads to unrealistic and conflicting outcomes. Whereas the historical trajectory of the target agents is quite informative most of the time, the interactions with other agents, traffic signals, and other environmental factors

are typically sparse and short in duration, but can be crucial when they occur. Second, although deep learning frameworks, especially graph neural networks and transformers, have led to recent progress, the black-box nature of state-of-the-art models makes it increasingly difficult to understand the contributing factors of a prediction model and their quantitative significance among all input variables.

Due to the dynamic and uncertain nature of real-world driving environments, accurately predicting the future trajectory of objects in the scene is essential. Traditional autonomous driving pipelines (Kato et al. 2018; Fan et al. 2018) often treat trajectory prediction as a separate module. This module receives inputs from the perception module and outputs predicted trajectories to the downstream planning module. However, this method has limitations in considering the global context and adapting to changing environments. Meanwhile, they usually lack the interpretation ability.

Justifying motion prediction for autonomous vehicle decisions through explanations is pivotal for comprehending black-box outcomes and fostering public trust (Omeiza et al. 2021; Atakishiyev et al. 2024). Several attempts have been made to employ attention visualization techniques for explaining deep learning-based autonomous driving models (Zablocki et al. 2021). (Kim and Canny 2017) utilized a CNN-based attention model with additional saliency filtering to highlight regions causally influencing future steering angles. (Hou et al. 2019) introduced a CNN-based attention model to track vehicles or pedestrians that the network needs to focus on. (Kim and Bansal 2020) integrated spatial attention, convolutional feature networks, and recurrent agent networks within an attention bottleneck architecture to enhance model interpretability for trajectory prediction. (Zhou et al. 2021) proposed imitation learning, combining CNNs and RNNs with attention mechanisms to infer meaningful trajectories for guided agents. However, most existing models provide intrinsic explainability, which is inherent in the interpretability of self-explanatory models, and provide only single-modal predictions.

In light of these challenges, we present a trajectory prediction model with better explainability, which is a conditional diffusion representation enhancement with improved shapley value to provide multimodal and explainable future tra-

jectories for a set of agents, named Traj-Explainer. In the Traj-Explainer, a Conditional Diffusion model is proposed to represent the scene multi-agent trajectory information. Furthermore, an improved shapley value is introduced to provide global and scenario explanations for the prediction. Our main contributions are:

- A Explainable Conditional Diffusion Multimodal Trajectory Prediction framework (Traj-Explainer) is proposed, which improves prediction performance while providing global and scenario explainability of the model.
- The proposed Traj-Explainer accurately predicts multiple potential future positions for all vehicles within a scene, incorporating interaction information among agents derived from the Conditional Diffusion model.
- Our study offers a thorough analysis of explainability for a trajectory decision model through scenario feature importance, global feature importance. The identified influential feature importance align with human driving experiences across various scenes, suggesting that the proposed model effectively learns predictive behaviors. Indicating the robustness of the model.
- We validate the efficacy of our method using the extensive real world Waymo, NGSIM, HighD, and MoCAD datasets. Experimental results demonstrate superior performance of our approach.

Related Work

Generative Models for Trajectory Prediction

Recently, considering the necessity of perceiving the trajectory of automated vehicles, several researches have been conducted based on the generative models. These methods usually execute the motion prediction by inferring conditional probabilities $p(s;c)$. For instance, HP-GAN (Barsoum, Kender, and Liu 2018) employed an enhanced Wasserstein GAN to learn a probability density function of future human poses conditioned on prior poses. Concurrently, methods like Conditional Variational Auto-Encoders (C-VAEs) (Oh and Peng 2022) and Normalizing Flows (Schöller and Knoll 2021) have demonstrated efficacy in learning these conditional probability density function for predicting future trajectories. Recent studies have explored diffusion models as an alternative for modeling conditional distributions of sequences, such as human motion poses (Zhang et al. 2024) and planning tasks (Janner et al. 2022). In a pertinent contribution, (Gu et al. 2022) applied diffusion models to capture uncertainties in pedestrian motion.

For these diffusion-based models, the multi-model information is captured by the cross-attention module. (Ngiam et al. 2021; Amirloo et al. 2022) took agent embedding as query, set map embedding as key and value, and conducted cross-attention module completing the interaction between map and agents track. (Varadarajan et al. 2022) performed state-of-the-art on the Argoverse Motion Forecasting Competition (Chang et al. 2019) based on designed attention interaction modules named multi-context gating (MCG). (Tang et al.

2022) proposed a general diffusion-like architectural module MnM, win 2nd place in the 2022 Waymo Open Dataset Motion Prediction Challenge (Schwall et al. 2020).

Explainable Analysis Methods

Deep learning systems have significantly advanced various aspects of our lives, yet their opaque nature presents challenges across many applications. The inability to provide explanations for decisions undermines trust in these systems. Consequently, a considerable amount of research has focused on developing explainable AI methods (Jin et al. 2022; Huang et al. 2023) to supplement network predictions with comprehensible explanations.

In the realm of practical explainable machine learning, there are two main approaches: opting for a straightforward, interpretable model structure and then training it, or training a sophisticated model and subsequently devising interpretable techniques to explain its decisions. These approaches categorize explainable machine learning models into intrinsic and post-hoc explainability (Moraffah et al. 2020). Intrinsic explainability pertains to models that are inherently interpretable (e.g., decision trees, rule-based models, linear models), while post-hoc explainability involves developing techniques to explain trained machine learning models. Depending on the scope, post-hoc explainability is further divided into global and local explainability. Global explainability aims to elucidate the overarching logic and internal workings of complex models, whereas local explainability seeks to clarify the decision-making process and rationale for individual input samples.

Methodology

In this section, we present our innovative Traj-Explainer framework designed to model intricate traffic scenarios while emphasizing feature importance. The framework is shown in Figure 1, including conditional diffusion model, scene encoding model, feature decoding model, and explanation analysis model.

Conditional Diffusion Model

As a traffic scene involves multiple traffic participants, a single-agent diffusion model (Yang et al. 2024) may generate sub-optimal samples when a scene involves significant interactions and uncertainties among multiple agents. To tackle this problem, we proposed a conditional diffusion to handle uncertainties and interaction. By modeling trajectories as diffusion processes, we can capture the stochastic and interaction nature of movement patterns and adapt to varying environmental conditions or unforeseen events. Our model operates on the history and future trajectories of all agents in a scene, and it thus can capture the spatial and temporal interaction among agents.

Figure 2 illustrates the structure of the Scenario Conditional Diffusion blocks responsible for encoding action latent information. In this architecture, the network is fed with random noise points, temporal sequences, and historical agent

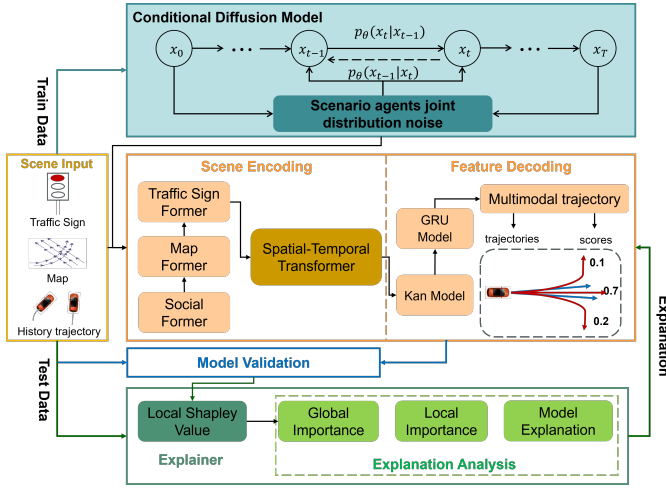


Figure 1: Overview of the Traj-Explainer framework.

trajectories as input, generating "scenario latent space" outputs directed to the scene encoder. To refine the diffusion network, we intricately design the loss function of Denoising Diffusion Probabilistic Models (DDPM) to guide the network towards producing action latent representations that comply with the kinematic constraints governing agent behaviors. This optimization not only ensures adherence to the physical laws governing agent movements but also augments the variability of their actions by embracing the inherent uncertainty within the data generated by the diffusion model. Note that trajectories are sampled at the scenario level instead of the agent level, as our model simultaneously predicts outcomes for all agents in a scene. This means our model can capture the interactions between agents in a scene.

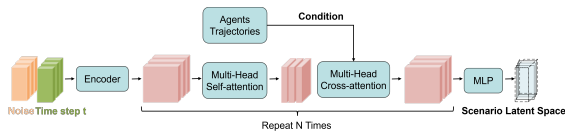


Figure 2: Overview of the developed conditional diffusion blocks for scenario latent space.

Scene Encoding

We utilize multiple embedding blocks with varying sizes and layers to effectively encode agents such as vehicles, bicycles, and pedestrians, alongside map and traffic sign data, ensuring the generation of diverse and realistic trajectories. These blocks are designed with a global capacity to capture comprehensive agent characteristics. This approach eliminates the need to convert the coordinate system into Frenet coordinates centered around individual agents, a conventional practice in existing trajectory prediction models.

Figure 3 illustrates the framework of the encoder. Each agent's positional and semantic embeddings are obtained individually and processed through a multilayer percep-

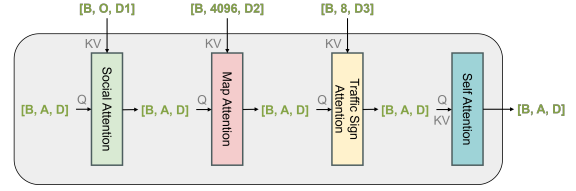


Figure 3: Overview of the encoder, Q - Queries, KV - Keys and Values, B - Batch size, A - Agent number, O - Neighbor agent number, D, D1, D2, D3 - Feature dimensions.

tron to derive a unified embedding. This embedding is then augmented with latent future embeddings acquired from a diffusion model, resulting in predicted agent embeddings of shape $[B, A, D]$. To further generate scene-level representations encompassing predicted agents, other agents, maps, and traffic signs, cross-attention mechanisms are applied between the embeddings of predicted agents and other agents. Subsequently, these embeddings undergo further cross-attention processes involving map embeddings sampled at points within each map polygon and traffic sign features represented as one-hot embeddings. These procedures ensure an accurate representation of traffic scenarios. More details are available in the **Appendix A**.

Spatial and Temporal Fusion Attention To effectively capture the complex dynamics of traffic scenarios, we introduce a Temporal Spatial Fusion Attention (TSFA) layer. This layer is specifically designed to integrate temporal and spatial characteristics inherent in the movements of predicted agents, leveraging multi-modal data that includes predicted agents, neighboring agents, map configurations, and traffic sign within traffic environments.

To enhance the description of movements, the TSFA layer enriches its features with "scenario latent features" information derived from a diffusion process. Multi-head self-attention blocks are employed to extract critical insights from the spatial-temporal data. These blocks play a crucial role in identifying essential spatial and temporal details within the broader context of multi-modal traffic scenes.

Feature Decoding

The trajectory decoder plays a crucial role in translating integrated traffic features into the future trajectories of agents. In this study, our decoder includes GRU blocks and KAN blocks, carefully configured to handle the temporal fluctuations inherent in agent movements. Inspired by the principles of multimodal trajectory prediction, which emphasize adaptability to agents exhibiting diverse behaviors over time, we introduce a multimodal output mechanism capable of effectively accommodating agents with varying actions in (Yang et al. 2024). More details and training objectives are provided in the **Appendix B**.

Explainability Analysis

In this study, we aim to deepen our understanding of the information utilized by trajectory generation models for effective performance. Specifically, we seek to quantify the

contribution of each input feature to the performance of a model (as opposed to its output).

Global and Scenario Feature Importance

Theorem 1. (Markov blanket) *Given a feature X_i , the subset $M \subseteq \setminus X_i$ is a Markov blanket of X_i if,*

$$p(\{F \setminus \{X_i, M\}, C\} | \{X_i, M\}) = p(\{F \setminus \{X_i, M\}, C\} | M) \quad (1)$$

This means that M contains all the information about C that X_i has about C . It is proved that strongly relevant features do not have a Markov blanket.

Theorem 2. (Chain rule for mutual information) *Given a set of random variables $X = \{X_1, X_2, \dots, X_n\}$ and random variable Y , then the mutual information of X and Y is defined as:*

$$\begin{aligned} I(X, Y) &= I(X_1, X_2, \dots, X_n; Y) \\ &= \sum_{y \in Y_{true}} \sum_{x \in X} p(x, y) \log \frac{p(x, y)}{p(x)p(y)} \\ &= \sum_{i=1}^n I(X_i; Y | X_{i-1}, X_{i-2}, \dots, X_1) \end{aligned} \quad (2)$$

The chain rule for mutual information indicates the amount of information that the random variables set X can provide for Y equals to the sum of pairwise mutual information of Y and each variable under certain conditions.

Definition 1. (Relative Feature Importance) *Let $X = (X_1, X_2, \dots, X_{N-1}, X_N)$ be the features of the to-be-predicted agent, and Y is ground truth of the future trajectories of the to-be-predicted agent. We define relative feature importance of $X_i \in X$ with respect to $X \setminus X_i$ as:*

$$RFI(X_i) = I(X_i; Y | X \setminus X_i) \quad (3)$$

$RFI(X_i)$ can be interpreted as the amount of reduced uncertainty of Y due to X_i given $X \setminus X_i$. $RFI(X_i) > 0$ means that X_i is conditional relevance to Y .

Definition 2. (Global Feature Importance) *Let $X = (X_1, X_2, \dots, X_{N-1}, X_N)$ be the features of the to-be-predicted agent, and Y is ground truth of the future trajectories of the to-be-predicted agent. From the perspective of information theory, the global feature importance of $X_i \in X$ is defined as,*

$$GFI(X_i) = I(X_i; Y) \quad (4)$$

$GFI(X_i)$ can be interpreted as the amount of reduced uncertainty of Y due to X_i . Global importance returns the overall impact of a feature on the model and is usually obtained by aggregating the feature attribution to the entire dataset. The higher the absolute value, the greater the impact of the feature on the model's predictions.

Definition 3. (Scenario Feature Importance) *Let $x_s = (x_1, x_2, \dots, x_{n-1}, x_n)$ be the features local values of the to-be-predicted agent, and y is ground truth of the future trajectories of the to-be-predicted agent in a specific scenario. The Scenario Feature Importance is defined as:*

$$SFI = I(x_i, y | x_s \setminus x_i) \quad (5)$$

Scenario importance returns feature attribution values for each explained scenario. These values describe how much a particular feature affects the prediction relative to the baseline prediction.

For a given dataset, scenario features are incorporated into global features, such as $x_i \in X_i$. In traffic scenes, history trajectories, neighboring agents, traffic signs, and maps align with the Markov blanket described in Theorem 1, indicating their strong relevance. Additionally, the relationship between these features and the target is relative, as features seldom exist independently, aligning with Definition 1. To evaluate the trajectory prediction model's representation capability, we define global feature importance (Definition 2) and scenario feature importance (Definition 3). Global feature importance is derived from relative feature importance, adhering to Theorem 2. However, computing high-dimensional conditional probability distributions is impractical, so we propose an approximated shapley value method for feature importance in the next subsection.

Implementation of Feature Importance Measure

Scenario Feature Importance Measure For trajectory prediction, we adjust the shapley value method by using a static, non-interacting agent as the baseline. This approach measures the contribution of a target agent's past trajectory relative to this static baseline. Contributions from neighboring agents, traffic sign, and map are evaluated against a scene where these elements are absent. Details of the shapley value implementation are provided in the Appendix.

Global Feature Importance Measure Here our challenge lies in determining each feature's overall contribution across the dataset, particularly when feature dynamics vary across scenarios (Makansi et al. 2021). To address this issue, we categorize features into two types: global and scenario features. Global features, like the agent's past trajectory and map data, remain constant across scenarios. For these, we adopt the conventional averaging approach to estimate their overall importance, termed as global feature importance. Conversely, scenario specific features, such as neighboring agents and traffic sign, exhibit variability across different scenes. To handle these, we employ a two-step aggregation process. Firstly, within each scenario, we locally aggregate the feature's impact using the max operator. This method effectively identifies the most influential neighboring agent or significant traffic sign within that scenario. Secondly, we globally aggregate these scenario specific contributions across the dataset using the average operator. This approach ensures that we capture meaningful insights into the collective influence of these features while accounting for their scenario-specific variability.

Experiment and Result Analysis

Evaluation Dataset

We train and evaluate our model on four large-scale real-world datasets. Waymo Motion Prediction dataset (Waymo) (Sun et al. 2021) contains 576,012 9-second sequences, each of which corresponds to a real trajectory sequence collected

Method		minSADE ↓	minSFDE ↓	sMR ↓	mAP ↑
Val	SceneTransformer(M)	1.12	2.60	0.54	0.09
	SceneTransformer(J)	0.97	2.17	0.49	0.12
	Wayformer	0.99	2.30	0.47	0.16
	MultiPath++	1.00	2.33	0.54	0.18
	JFP	0.87	1.96	0.42	0.20
	MotionDiffuser	0.86	1.92	0.42	0.19
	Traj-Explainer(ours)	0.849	1.71	0.44	0.18
Test	MultiPath++	1.00	2.33	0.54	0.17
	JFP	0.88	1.99	0.42	0.21
	MotionDiffuser	0.86	1.95	0.43	0.20
	Traj-Explainer(ours)	0.85	1.74	0.42	0.20

Table 1: Evaluation of multimodal motion prediction capability on scene level joint metrics

from the corresponding driving scene at a frequency of 10 Hz. Among them, (0,1] seconds are used for observation and (1,9] seconds are used for prediction. NGSIM (Deo and Trivedi 2018), HighD (Krajewski et al. 2018), and MoCAD (Liao et al. 2024b) are three mainstream trajectory prediction datasets, which are derived from a variety of complex real-world traffic conditions such as highways, and urban areas, and serve as comprehensive testing grounds. Following the general dataset partitioning framework. The trajectory is divided into 8 segments, of which the first 3 seconds are used as historical data and the following 5 seconds are used for evaluation. For these three datasets, 70% of the data are used for training, 10% for evaluation, and 20% for testing.

Evaluation Metrics

We use the widely adopted official indicators. For Waymo dataset, we evaluate our model’s performance using the Waymo Motion Prediction metrics. Following the standard evaluation protocol, we adopt The Minimum Average Displacement Error (minSADE), the Minimum Final Displacement Error (minSFDE), Missing Rate(sMR) and Mean average precision (mAP) for evaluation, which are defined in (Ettinger et al. 2021). These metrics serve as benchmarks to gauge the accuracy and reliability of our model’s trajectory predictions against the Waymo dataset.

For NGSIM, HighD, and MoCAD datasets, we evaluate the results with RMSE over a 5-second prediction time, which keeps consistent with the evaluation indicators in the mainstream methods. For multimodal methods, we select the predicted trajectory corresponding to the maneuver with the highest probability.

Quantitative Analysis

To evaluate Traj-Explainer’s performance in multimodal trajectory prediction settings, we conduct our method against a range of leading-edge benchmarks on the Waymo dataset.

Table 1 presents the primary metrics for multimodal trajectory prediction on the Waymo dataset. We evaluate Traj-Explainer against various SOTA multimodal trajectory prediction methods, including SceneTransformer(M) (Ngiam et al. 2021), SceneTransformer(J) (Ngiam et al. 2021), Wayformer (Nayakanti et al. 2023), MultiPath++ (Varadarajan et al. 2022), JFP (Luo et al. 2023), MotionDiffuser (Ngiam

Dataset	Model	Prediction Time				
		1s	2s	3s	4s	5s
NGSIM	MATF-GAN	0.66	1.34	2.08	2.97	4.13
	NLS	0.56	1.22	2.02	3.03	4.30
	DRBP	1.18	2.83	4.22	5.82	-
	DN-IRL	0.54	1.02	1.91	2.43	3.76
	WSiP	0.56	1.23	2.05	3.08	4.34
	CF-LSTM	0.55	1.10	1.78	2.73	3.82
	MHA	0.41	1.01	1.74	2.67	3.83
	HMNet	0.50	1.13	1.89	2.85	4.04
	TS-GAN	0.60	1.24	1.95	2.78	3.72
	STDAN	0.39	0.96	1.61	2.56	3.67
	BAT	0.23	0.81	1.54	2.52	3.62
	Traj-Explainer(ours)	0.22	0.85	1.53	2.49	3.60
	WSiP	0.20	0.60	1.21	2.07	3.14
	MHA	0.19	0.55	1.10	1.84	2.78
highD	NLS	0.20	0.57	1.14	1.90	2.91
	DRBP	0.41	0.79	1.11	1.40	-
	EA-Net	0.15	0.26	0.43	0.78	1.32
	CF-LSTM	0.18	0.42	1.07	1.72	2.44
	STDAN	0.19	0.27	0.48	0.91	1.66
	iNATran	0.04	0.05	0.21	0.54	1.10
	BAT	0.08	0.14	0.20	0.44	0.62
	Traj-Explainer(ours)	0.09	0.12	0.19	0.42	0.65
MoCAD	S-GAN	1.69	2.25	3.30	3.89	4.69
	CS-LSTM	1.45	1.98	2.94	3.56	4.49
	MHA	1.25	1.48	2.57	3.22	4.20
	NLS	0.96	1.27	2.08	2.86	3.93
	WSiP	0.70	0.87	1.70	2.56	3.47
	CF-LSTM	0.72	0.91	1.73	2.59	3.44
	STDAN	0.62	0.85	1.62	2.51	3.32
	BAT	0.35	0.74	1.39	2.19	2.88
	Traj-Explainer(ours)	0.37	0.71	1.42	2.10	2.76

Table 2: Comparison results between baselines and our proposed method.

et al. 2021). While MotionDiffuser and our model are both diffusion-based approaches, our method outperforms significantly across all metrics, attributed to the robustness of our overall structure, with the exception of sMR. In comparison to JFP on both validation and test datasets, our model shows improvements in metrics such as minSADE, minSFDE, and mAP. More results on the Waymo dataset are available in the **Appendix C**.

In addition, we evaluate Traj-Explainer against several state-of-the-art (SOTA) trajectory prediction methods on the NGSIM, highD, and MoCAD datasets, as detailed in Table 2. These methods include well-established benchmarks such as MATF-GAN (Zhao et al. 2019), NLS (Messaoud et al. 2019), DN-IRL (Fernando et al. 2019), DRBP (Gao et al. 2023), WSiP (Wang et al. 2023), CF-LSTM (Xie et al. 2021), MHA (Messaoud et al. 2020), MATH (Hasan et al. 2021), HMNet (Xue et al. 2021), EA-Net (Chen et al. 2022a), TS-GAN (Wang et al. 2020), STDAN (Chen et al. 2022b), iNATran (Chen et al. 2022a) and BAT (Liao et al. 2024a). Our model demonstrates a significant improvement over existing SOTA baselines. Specifically, it surpasses BAT by 1.46% in the 1-5s range. On the NGSIM dataset, our model is comparable to BAT in 1-3s predictions but outperforms BAT in long-term predictions (4-5s). For the highD dataset, known for its large data volume and accuracy, our model performs notably better than most baselines and matches BAT’s performance. Furthermore, compared to STDAN, our method achieves improvements of 69.2% and 20.29% in the 5s prediction range on the highD and MoCAD datasets, respectively.

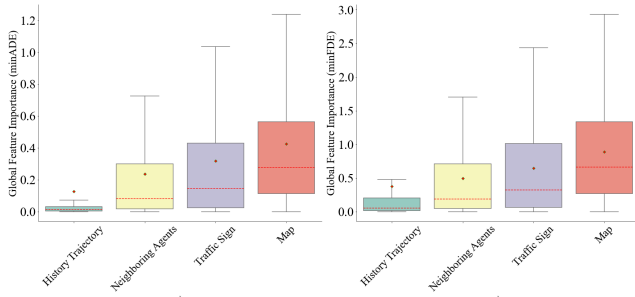


Figure 4: Global feature importance (Shapley Value). The red dot represents the mean value and the red dashed line represents the median.

Explainability Analysis

This paper discusses the impact of history trajectory, neighboring agents, traffic sign, and map features on the performance of the prediction algorithm. The minADE and minFDE are used as shapley error metrics. The prediction model is trained on the Waymo training set, and explainability analysis is performed on its test set.

Global Feature Importance Figure 4 shows the feature importance of minADE error and minFDE error. The results show that the map feature is the most important, followed by the traffic sign, neighboring agents and history trajectory. This order of importance is consistent with human driving behavior cognition, indicating that our model has learned the correct feature semantics. You may question why the historical trajectory has the lowest importance. In fact, it is reasonable, because the history trajectory trajectories are strongly correlated features, but are weakly correlated features when a map is given., that is, trajectory trajectories are redundant features given map, which also shows that our model has learned the redundant relationship between features.

Scenario Feature Importance Figure 5 shows the importance of traffic sign under different scenario modes. It can be seen that the importance of traffic sign in the case of stopping, turning left, and turning right is relatively large, and the importance is the smallest in the case of irregular road. The reasons may be as follows: stopping, turning left, and turning right are all carried out near the intersection roads, and their decisions are closely related to traffic sign. For example, turning right needs to consider the straight and left turn signals, and stopping will be affected by opposite signals and multiple crosswalks. In addition, irregular road generally have few traffic signs, so the corresponding features are the least important. The importance analysis of history trajectory, neighboring agents, and map are provided in the **Appendix D**.

Figure 6 illustrates the prediction outcomes of the proposed framework across various scenarios, with each row depicting a distinct traffic environment. Specifically, four scenarios are presented: lane keeping, stop-start, turning, and interaction scenarios. In the first row of Figure 6, which pertains to lane keeping situations, predictions typically exhibit high cogni-

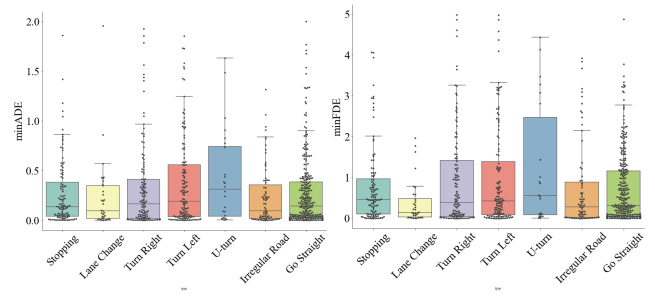


Figure 5: The results of the trajectory prediction error under different traffic scenario caused by traffic sign.

Spatial&Temporal Attention	Social Former	Map Former	Traffic Sign Former	minSADE↓	minSFDE↓
✓	✓	✓	✓	1.122	1.993
✓	✓	✓	✓	1.025	1.798
✓	✓	✓	✓	1.245	2.062
✓	✓	✓	✓	1.084	1.887
✓	✓	✓	✓	0.850	1.740

Table 3: Ablation study on the scene encoding

tive certainty. Here, the vehicle’s future trajectory is largely influenced by map. Conversely, the second and third rows depict scenarios characterized by significant trajectory prediction errors, often accompanied by heightened cognitive uncertainty estimates. This occurs when vehicles approach intersections or experience substantial changes in movement patterns or speed compared to their historical trajectories. In stop start scenario, future decisions are less correlated with historical trajectories and more dependent on factors like neighboring agents, traffic sign and map information. In the turning scenario, future trajectory are highly related to history trajectory, and this scenario has the highest feature importance of history trajectory, at 8.204, which means history trajectory are essential for future predictions. This is also consistent with human cognition, because the map lines are discontinuous at turns, and future predictions will rely more on history trajectory. The last row showcases irregular intersections or road sections, where predictions are marked by the highest cognitive uncertainty. Here, the vehicle’s future state is influenced by neighboring agents and map, with minimal reliance on traffic sign or history trajectory.

These results underscore conditional correlations between history trajectory and map, highlighting instances where these features exhibit redundancy in predicting future trajectories. Moreover, our model effectively learns and reflects this redundancy in its scenario feature importance rankings. For instance, in the first row of Figure 6, either map features or history trajectory exhibit lower importance depending on the scenario. We also reached the same conclusion in terms of global feature importance. This confirms that our model is not only globally robust but also locally robust.

Ablation Studies on Traffic Scene Encoding

In this subsection, we assess the structural impact by adding or removing components of the traffic scene encoder, which includes spatial and temporal attention modules, social for-

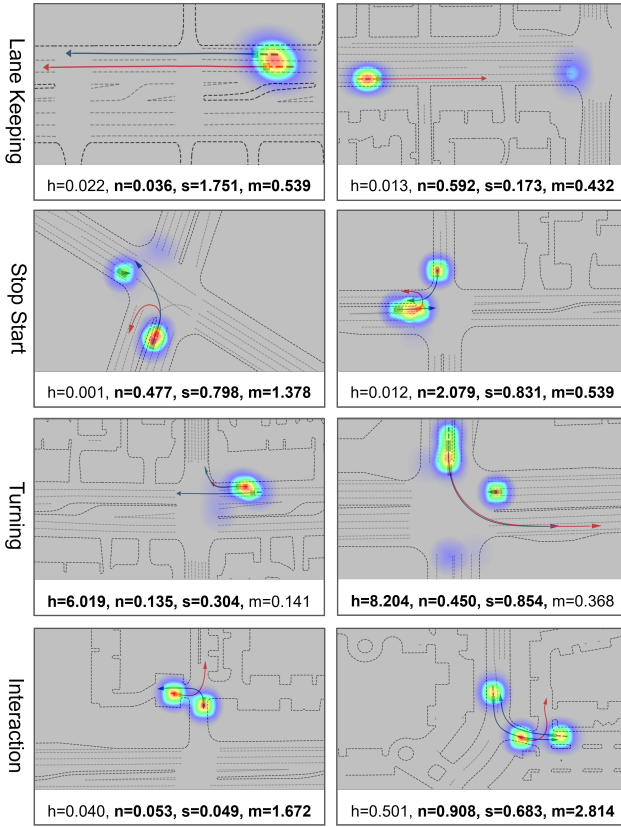


Figure 6: Qualitative results of trajectory prediction and feature importance estimation on different scenarios (corresponding to different rows). Different colors are used to denote different agents: red - predicted agent; blue - neighbor agents. The dotted line represents the historical trajectory, and the solid line represents the future trajectory. In addition, the scenario feature importance is highlighted in heatmap. h , n , s , m represent the feature importance of history trajectory, neighboring agents, traffic sign and map respectively.

mer, map former, and traffic light former. We utilize minSADE and minSFDE metrics to evaluate the alignment of generated trajectories with ground truth.

Table 3 presents the evaluation results, highlighting the critical role of the map former in accurate trajectory generation. Without this module, the model shows its poorest minSADE and minSFDE performances, indicating its crucial role in ensuring compliance with lane constraints during trajectory generation. Similarly, the spatial and temporal attention modules are essential, significantly enhancing the scene encoder’s understanding of traffic scenarios. Their absence results in minSADE and minSFDE scores of 1.122 and 1.993, respectively, below optimal levels. The traffic sign module also proves crucial, as its absence negatively impacts trajectory accuracy to a degree comparable to missing spatial and temporal attention modules. Additionally, social former modules play a significant role in integrating the historical movements of neighboring agents, which is crucial for gen-

MLP	KAN	GRU Blocks	minSADE↓	minSFDE↓
		✓	1.990	2.857
	2 Layers		0.892	2.170
1 Layer		✓	0.861	1.803
2 Layers		✓	0.855	1.783
	1 Layer	✓	0.859	1.750
	2 Layers	✓	0.850	1.740

Table 4: Ablation study on the multimodal trajectory decoding

erating safe trajectories.

Combining all these modules, our traffic scene encoder achieves optimal performance, reflected in the lowest minSADE and minSFDE scores, demonstrating the effectiveness of our comprehensive approach in encoding the surrounding environment.

Ablation Studies on Trajectory Decoding

In this subsection, we evaluate the architecture of the trajectory decoder, with a specific focus on GRU (Gated Recurrent Unit) blocks and KANblocks. This evaluation aims to ascertain how each component and configuration impacts the decoder’s ability to accurately predict future trajectories, emphasizing their critical role in enhancing model performance.

Table 4 presents the evaluation results, highlighting the pivotal role of KANlayers in the trajectory decoder’s performance. The absence of KANblocks significantly deteriorates results, with the model achieving the highest minSADE and minSFDE scores of 1.990 and 2.857, respectively. This performance decline is attributed to the fundamental role of KANblocks in improving the decoder’s prediction capabilities and handling, integrating complex features extracted from input data. Additionally, the importance of GRU blocks is underscored, enabling the decoder to effectively utilize historical information and further contribute to accurate future trajectory predictions. Combining KAN and GRU blocks, our model achieves optimal results, demonstrating outstanding trajectory prediction with the lowest minSADE and minSFDE scores. Furthermore, we compared the performance of the KAN model and MLP model with experimental settings and results summarized in Table 4. It is evident that the Kan model with 2 layers achieved the best performance.

Conclusion

In this study, we introduce Traj-Explainer, a novel approach for Explainable Conditional Diffusion-based Multimodal Trajectory Prediction. Our method, Traj-Explainer, incorporates an advanced conditional diffusion technique to model diverse trajectory patterns. Additionally, we enhance the shapley value model to better understand global and scenario-specific feature importance. Through extensive evaluations, we demonstrate the effectiveness of our approach on several benchmarks compared to other baselines. Future research directions involve extending the diffusion-

based generative modeling technique to address other pertinent areas in autonomous vehicles, including planning conditional trajectory generation. We can also extend the framework for pedestrian trajectory prediction.

References

- Amirloo, E.; Rasouli, A.; Lakner, P.; Rohani, M.; and Luo, J. 2022. LatentFormer: Multi-Agent Transformer-Based Interaction Modeling and Trajectory Prediction. *arXiv preprint arXiv:2203.01880*.
- Atakishiyev, S.; Salameh, M.; Yao, H.; and Goebel, R. 2024. Explainable artificial intelligence for autonomous driving: A comprehensive overview and field guide for future research directions. *IEEE Access*.
- Barsoum, E.; Kender, J.; and Liu, Z. 2018. Hp-gan: Probabilistic 3d human motion prediction via gan. In *Proceedings of the IEEE conference on computer vision and pattern recognition workshops*, 1418–1427.
- Chang, M.-F.; Lambert, J.; Sangkloy, P.; Singh, J.; Bak, S.; Hartnett, A.; Wang, D.; Carr, P.; Lucey, S.; Ramanan, D.; et al. 2019. Argoverse: 3d tracking and forecasting with rich maps. In *Proceedings of the IEEE/CVF conference on computer vision and pattern recognition*, 8748–8757.
- Chen, X.; Zhang, H.; Zhao, F.; Cai, Y.; Wang, H.; and Ye, Q. 2022a. Vehicle trajectory prediction based on intention-aware non-autoregressive transformer with multi-attention learning for Internet of Vehicles. *IEEE Transactions on Instrumentation and Measurement*, 71: 1–12.
- Chen, X.; Zhang, H.; Zhao, F.; Hu, Y.; Tan, C.; and Yang, J. 2022b. Intention-aware vehicle trajectory prediction based on spatial-temporal dynamic attention network for internet of vehicles. *IEEE Transactions on Intelligent Transportation Systems*, 23(10): 19471–19483.
- Deo, N.; and Trivedi, M. M. 2018. Convolutional social pooling for vehicle trajectory prediction. In *Proceedings of the IEEE conference on computer vision and pattern recognition workshops*, 1468–1476.
- Ettinger, S.; Cheng, S.; Caine, B.; Liu, C.; Zhao, H.; Pradhan, S.; Chai, Y.; Sapp, B.; Qi, C. R.; Zhou, Y.; et al. 2021. Large scale interactive motion forecasting for autonomous driving: The waymo open motion dataset. In *Proceedings of the IEEE/CVF International Conference on Computer Vision*, 9710–9719.
- Fan, H.; Zhu, F.; Liu, C.; Zhang, L.; Zhuang, L.; Li, D.; Zhu, W.; Hu, J.; Li, H.; and Kong, Q. 2018. Baidu apollo em motion planner. *arXiv preprint arXiv:1807.08048*.
- Feng, C.; Zhou, H.; Lin, H.; Zhang, Z.; Xu, Z.; Zhang, C.; Zhou, B.; and Shen, S. 2023. Macformer: Map-agent coupled transformer for real-time and robust trajectory prediction. *IEEE Robotics and Automation Letters*.
- Fernando, T.; Denman, S.; Sridharan, S.; and Fookes, C. 2019. Neighbourhood context embeddings in deep inverse reinforcement learning for predicting pedestrian motion over long time horizons. In *Proceedings of the IEEE/CVF International Conference on Computer Vision Workshops*, 0–0.
- Gao, K.; Li, X.; Chen, B.; Hu, L.; Liu, J.; Du, R.; and Li, Y. 2023. Dual transformer based prediction for lane change intentions and trajectories in mixed traffic environment. *IEEE Transactions on Intelligent Transportation Systems*, 24(6): 6203–6216.
- Gu, T.; Chen, G.; Li, J.; Lin, C.; Rao, Y.; Zhou, J.; and Lu, J. 2022. Stochastic trajectory prediction via motion indeterminacy diffusion. In *Proceedings of the IEEE/CVF Conference on Computer Vision and Pattern Recognition*, 17113–17122.
- Hasan, M.; Solernou, A.; Paschalidis, E.; Wang, H.; Markkula, G.; and Romano, R. 2021. Maneuver-aware pooling for vehicle trajectory prediction. *arXiv preprint arXiv:2104.14079*.
- Hou, L.; Xin, L.; Li, S. E.; Cheng, B.; and Wang, W. 2019. Interactive trajectory prediction of surrounding road users for autonomous driving using structural-LSTM network. *IEEE Transactions on Intelligent Transportation Systems*, 21(11): 4615–4625.
- Huang, W.; Zhao, X.; Jin, G.; and Huang, X. 2023. Safari: Versatile and efficient evaluations for robustness of interpretability. In *Proceedings of the IEEE/CVF International Conference on Computer Vision*, 1988–1998.
- Janner, M.; Du, Y.; Tenenbaum, J. B.; and Levine, S. 2022. Planning with diffusion for flexible behavior synthesis. *arXiv preprint arXiv:2205.09991*.
- Jin, G.; Yi, X.; Huang, W.; Schewe, S.; and Huang, X. 2022. Enhancing adversarial training with second-order statistics of weights. In *Proceedings of the IEEE/CVF conference on computer vision and pattern recognition*, 15273–15283.
- Kato, S.; Tokunaga, S.; Maruyama, Y.; Maeda, S.; Hirabayashi, M.; Kitsukawa, Y.; Monroy, A.; Ando, T.; Fujii, Y.; and Azumi, T. 2018. Autoware on board: Enabling autonomous vehicles with embedded systems. In *2018 ACM/IEEE 9th International Conference on Cyber-Physical Systems (ICCPS)*, 287–296. IEEE.
- Kim, J.; and Bansal, M. 2020. Attentional bottleneck: Towards an interpretable deep driving network. In *Proceedings of the IEEE/CVF Conference on Computer Vision and Pattern Recognition Workshops*, 322–323.
- Kim, J.; and Canny, J. 2017. Interpretable learning for self-driving cars by visualizing causal attention. In *Proceedings of the IEEE international conference on computer vision*, 2942–2950.
- Krajewski, R.; Bock, J.; Kloeker, L.; and Eckstein, L. 2018. The highd dataset: A drone dataset of naturalistic vehicle trajectories on german highways for validation of highly automated driving systems. In *2018 21st international conference on intelligent transportation systems (ITSC)*, 2118–2125. IEEE.
- Liao, H.; Li, Z.; Shen, H.; Zeng, W.; Liao, D.; Li, G.; and Xu, C. 2024a. Bat: Behavior-aware human-like trajectory prediction for autonomous driving. In *Proceedings of the AAAI Conference on Artificial Intelligence*, volume 38, 10332–10340.
- Liao, H.; Shen, H.; Li, Z.; Wang, C.; Li, G.; Bie, Y.; and Xu, C. 2024b. Gpt-4 enhanced multimodal grounding for

- autonomous driving: Leveraging cross-modal attention with large language models. *Communications in Transportation Research*, 4: 100116.
- Liebel, L.; and Körner, M. 2018. Auxiliary tasks in multi-task learning. *arXiv preprint arXiv:1805.06334*.
- Luo, W.; Park, C.; Cornman, A.; Sapp, B.; and Anguelov, D. 2023. Jfp: Joint future prediction with interactive multi-agent modeling for autonomous driving. In *Conference on Robot Learning*, 1457–1467. PMLR.
- Makansi, O.; Von Kügelgen, J.; Locatello, F.; Gehler, P.; Janzing, D.; Brox, T.; and Schölkopf, B. 2021. You mostly walk alone: Analyzing feature attribution in trajectory prediction. *arXiv preprint arXiv:2110.05304*.
- Messaoud, K.; Yahiaoui, I.; Verroust-Blondet, A.; and Nashashibi, F. 2019. Non-local social pooling for vehicle trajectory prediction. In *2019 IEEE Intelligent Vehicles Symposium (IV)*, 975–980. IEEE.
- Messaoud, K.; Yahiaoui, I.; Verroust-Blondet, A.; and Nashashibi, F. 2020. Attention based vehicle trajectory prediction. *IEEE Transactions on Intelligent Vehicles*, 6(1): 175–185.
- Montali, N.; Lambert, J.; Mougin, P.; Kuefler, A.; Rhinehart, N.; Li, M.; Gulino, C.; Emrich, T.; Yang, Z.; Whiteson, S.; et al. 2023. The waymo open sim agents challenge. *arXiv preprint arXiv:2305.12032*.
- Moraffah, R.; Karami, M.; Guo, R.; Raglin, A.; and Liu, H. 2020. Causal interpretability for machine learning-problems, methods and evaluation. *ACM SIGKDD Explorations Newsletter*, 22(1): 18–33.
- Nayakanti, N.; Al-Rfou, R.; Zhou, A.; Goel, K.; Refaat, K. S.; and Sapp, B. 2023. Wayformer: Motion forecasting via simple & efficient attention networks. In *2023 IEEE International Conference on Robotics and Automation (ICRA)*, 2980–2987. IEEE.
- Ngiam, J.; Caine, B.; Vasudevan, V.; Zhang, Z.; Chiang, H.-T. L.; Ling, J.; Roelofs, R.; Bewley, A.; Liu, C.; Venugopal, A.; et al. 2021. Scene Transformer: A unified architecture for predicting multiple agent trajectories. *arXiv preprint arXiv:2106.08417*.
- Oh, G.; and Peng, H. 2022. Cvae-h: Conditionalizing variational autoencoders via hypernetworks and trajectory forecasting for autonomous driving. *arXiv preprint arXiv:2201.09874*.
- Omeiza, D.; Webb, H.; Jirotko, M.; and Kunze, L. 2021. Explanations in autonomous driving: A survey. *IEEE Transactions on Intelligent Transportation Systems*, 23(8): 10142–10162.
- Schöller, C.; and Knoll, A. 2021. Flomo: Tractable motion prediction with normalizing flows. In *2021 IEEE/RSJ International Conference on Intelligent Robots and Systems (IROS)*, 7977–7984. IEEE.
- Schwall, M.; Daniel, T.; Victor, T.; Favaro, F.; and Hohnhold, H. 2020. Waymo public road safety performance data. *arXiv preprint arXiv:2011.00038*.
- Shi, S.; Jiang, L.; Dai, D.; and Schiele, B. 2024. Mtr++: Multi-agent motion prediction with symmetric scene modeling and guided intention querying. *IEEE Transactions on Pattern Analysis and Machine Intelligence*.
- Sun, Z.; Wang, J.; Chen, Y.; Xu, J.; Zhang, X.; Li, Y.; Zhang, Y.; Liu, Z.; Guo, J.; Huang, T.; et al. 2021. Large scale interactive motion forecasting for autonomous driving: The waymo open motion dataset. In *Proceedings of the IEEE/CVF International Conference on Computer Vision*, 11271–11281.
- Tang, X.; Eshkevari, S. S.; Chen, H.; Wu, W.; Qian, W.; and Wang, X. 2022. Golfer: Trajectory Prediction with Masked Goal Conditioning MnM Network. *arXiv preprint arXiv:2207.00738*.
- Varadarajan, B.; Hefny, A.; Srivastava, A.; Refaat, K. S.; Nayakanti, N.; Cornman, A.; Chen, K.; Douillard, B.; Lam, C. P.; Anguelov, D.; et al. 2022. Multipath++: Efficient information fusion and trajectory aggregation for behavior prediction. In *2022 International Conference on Robotics and Automation (ICRA)*, 7814–7821. IEEE.
- Wang, R.; Wang, S.; Yan, H.; and Wang, X. 2023. Wsip: Wave superposition inspired pooling for dynamic interactions-aware trajectory prediction. In *Proceedings of the AAAI Conference on Artificial Intelligence*, volume 37, 4685–4692.
- Wang, Y.; Zhao, S.; Zhang, R.; Cheng, X.; and Yang, L. 2020. Multi-vehicle collaborative learning for trajectory prediction with spatio-temporal tensor fusion. *IEEE Transactions on Intelligent Transportation Systems*, 23(1): 236–248.
- Wang, Y.; Zhao, T.; and Yi, F. 2023. Multiverse transformer: 1st place solution for waymo open sim agents challenge 2023. *arXiv preprint arXiv:2306.11868*.
- Xie, X.; Zhang, C.; Zhu, Y.; Wu, Y. N.; and Zhu, S.-C. 2021. Congestion-aware multi-agent trajectory prediction for collision avoidance. In *2021 IEEE International Conference on Robotics and Automation (ICRA)*, 13693–13700. IEEE.
- Xue, Q.; Li, S.; Li, X.; Zhao, J.; and Zhang, W. 2021. Hierarchical motion encoder-decoder network for trajectory forecasting. *arXiv preprint arXiv:2111.13324*.
- Yang, C.; Tian, A. X.; Chen, D.; Shi, T.; and Heydarian, A. 2024. WcDT: World-centric Diffusion Transformer for Traffic Scene Generation. *arXiv preprint arXiv:2404.02082*.
- Zablocki, É.; Ben-Younes, H.; Pérez, P.; and Cord, M. 2021. Explainability of vision-based autonomous driving systems: Review and challenges. *arXiv preprint arXiv:2101.05307*, 2.
- Zhang, M.; Cai, Z.; Pan, L.; Hong, F.; Guo, X.; Yang, L.; and Liu, Z. 2024. Motiandiffuse: Text-driven human motion generation with diffusion model. *IEEE Transactions on Pattern Analysis and Machine Intelligence*.
- Zhao, T.; Xu, Y.; Monfort, M.; Choi, W.; Baker, C.; Zhao, Y.; Wang, Y.; and Wu, Y. N. 2019. Multi-agent tensor fusion for contextual trajectory prediction. In *Proceedings of the IEEE/CVF conference on computer vision and pattern recognition*, 12126–12134.

Zhou, J.; Wang, R.; Liu, X.; Jiang, Y.; Jiang, S.; Tao, J.; Miao, J.; and Song, S. 2021. Exploring imitation learning for autonomous driving with feedback synthesizer and differentiable rasterization. In *2021 IEEE/RSJ International Conference on Intelligent Robots and Systems (IROS)*, 1450–1457. IEEE.

Zhou, Z.; Wang, J.; Li, Y.-H.; and Huang, Y.-K. 2023. Query-centric trajectory prediction. In *Proceedings of the IEEE/CVF Conference on Computer Vision and Pattern Recognition*, 17863–17873.

Appendix A

Positional and Semantic Embedding The Positional Embedding consolidates all positional attributes, denoted as p_i , into a unified one-dimensional matrix. Simultaneously, the Feature-Embedding translates the agent’s characteristics, such as height, width, and type, represented in a one-hot encoding format into a corresponding one-dimensional matrix. For each predicted agent i ,

$$P_i = f_p(x_i, y_i) \quad (6)$$

where f_p represents a linear transformation layer, and P_i denotes the positional embedding result. The semantic embedding is denoted as:

$$F_i = f_f(f_w, f_h, f_{type}) \quad (7)$$

where f_f indicates a linear transformation layer, with f_w , f_h and f_{type} representing the agent’s width, height and type, respectively, the agent’s type is converted to a one hot encoded format. After that, to obtain a comprehensive representation of each agent, the position and feature embedding are synthesized by using a ReLU activation function, which is defined as:

$$R_i = \text{ReLU}(\text{LayerNorm}(\text{concat}(P_i, F_i))) \quad (8)$$

Appendix B

To mitigate the influence of agents’ initial positions on outcomes, our model outputs include move statements for agents along with their corresponding likelihoods. For agent i , the formulation of the trajectory in our model is expressed as follows:

$$\text{traj}_i = \text{pos}_{cur} + \sum_{t=cur}^T (\delta x, \delta y, \delta \sigma) \quad (9)$$

where pos_{cur} is the current position of agent i , traj_i represents the agent’s future trajectory points for time step T .

Training Objectives

Regression Loss Huber loss is a commonly used loss function for constraining the prediction. In our work, we inject diffusion generation information to increase the prediction’s interaction ability and diversity. The trajectory with minimal loss is selected, and its deviation from the ground truth is quantified using the Huber loss.

$$L_{reg} = \text{Huber}(\hat{s}_i, s_i) \quad (10)$$

Confidence loss To score the proposed region based on the probability of driving intention, we utilize the Kullback-Leibler Divergence as our loss function. This loss function restricts the contribution of probabilities from the proposals based on the distance between the predicted trajectory and ground truth.

$$L_{conf} = \frac{1}{N} \sum_{j=1}^N D_{KL}(\lambda(\hat{s}_i) || \gamma(s_i)) \quad (11)$$

where $\lambda(x_i)$ is the distribution of predicted proposals, $\gamma(y_i)$ is the distribution of ground-truth proposals.

Classification loss We cluster all endpoint coordinates into K categories and label the ground truth and prediction proposals with the nearest cluster centroid category label. We employ cross-entropy as an additional loss function to enhance the capability of predicting the driving intention of the vehicle.

$$L_{cls} = \frac{1}{N} \sum_{j=1}^N \text{CrossEntropy}(p(s_i), p(s_i)) \quad (12)$$

where $p(\hat{s}_i)$ is the probability distribution of predicted proposals, $p(s_i)$ is the ground-truth distribution of ground-truth proposals.

Hence, We formulate the loss as a sum of multiple task loss and use an auxiliary learning (Liebel and Körner 2018) approach to balance them.

$$L_{sum} = \frac{1}{\alpha_1^2} L_{reg} + \frac{1}{\alpha_2^2} L_{conf} + \frac{1}{\alpha_3^2} L_{cls} + \frac{1}{\alpha_4^2} L_{diff} + \sum_{i=1}^4 \log(\alpha_i + 1) \quad (13)$$

where L_{diff} is the L2 loss of the predicted noise and the original noise that is the standard diffusion model loss function. $\alpha_i, i = 1, 2, 3, 4$ are learnable weights.

Appendix C

In Table 5, we consult the Sim Agents Challenge metrics (Montali et al. 2023) on Waymo dataset to assess the realism and diversity of the trajectories generated by our model. These metrics comprehensively evaluate three critical aspects: kinematic Our framework demonstrates enhanced performance across all metrics compared to benchmarks such as Random Agent (Montali et al. 2023), Constant Velocity (Montali et al. 2023), MTR+++ (Shi et al. 2024), WayFormer (Nayakanti et al. 2023), and MULTIPATH+++ (Varadarajan et al. 2022). Although not consistently optimal against MVTA (Wang, Zhao, and Yi 2023) and MVTE (Wang, Zhao, and Yi 2023) in all individual indicators, our method shows improvement in the composite metric, which integrates multiple metrics. The Random Agent exhibits the poorest performance with the lowest composite metric score of 0.163, attributable to its random trajectory generation. In

Method	Linear Speed \uparrow	Linear Accel \uparrow	Ang Speed \uparrow	Ang Accel \uparrow	Dist to Obj \uparrow	Collision \uparrow	TTC \uparrow	Dist to Road Edge \uparrow	Offroad \uparrow	Composite Metric \uparrow	ADE \downarrow	minADE \downarrow
Random Agent	0.002	0.044	0.074	0.120	0.000	0.006	0.734	0.178	0.325	0.163	50.740	50.707
Constant Velocity	0.074	0.058	0.019	0.035	0.208	0.202	0.737	0.454	0.325	0.238	7.924	7.924
MTR+++	0.412	0.107	0.484	0.437	0.346	0.414	0.797	0.654	0.577	0.470	2.129	1.682
WayFormer	0.408	0.127	0.473	0.437	0.358	0.403	0.810	0.645	0.589	0.472	2.588	1.694
MULTIPATH++	0.432	0.230	0.515	0.452	0.344	0.420	0.813	0.639	0.583	0.489	5.308	2.052
MVTA	0.437	0.220	0.533	0.481	0.373	0.436	0.830	0.654	0.629	0.509	3.938	1.870
MVTE	0.443	0.222	0.535	0.481	0.382	0.451	0.832	0.664	0.641	0.517	3.873	1.677
Traj-Explainer(ours)	0.446	0.270	0.539	0.471	0.390	0.475	0.798	0.667	0.622	0.518	2.185	1.605

Table 5: Evaluation on kinematic metrics, object interaction metrics, and map-based metrics

contrast, Constant Velocity achieves a slightly higher composite metric of 0.238 due to its consideration of previous heading and speed information, significantly improving ADE and MinADE by over 40%. Notably, our method achieves the highest composite metric score of 0.518, indicating robust performance across all evaluated methods. This underscores our model’s advanced capability in accurately representing and interpreting dynamic traffic environment variables, showcasing its efficacy in trajectory prediction tasks on the Waymo dataset.

Appendix D

Figure 7 shows the importance results of history trajectory under different scenario modes. It can be seen that the importance of U-turn, go straight and irregular road is relatively large, while the importance of Turn Right and lane change is relatively small. The reasons may be as follows: First, turn right and lane change rely relatively more on map information; second, compared with turn left and go straight, vehicles are less affected by traffic lights and other signals when turning right, resulting in higher driving speeds. In addition, U-turns represent typical extreme cases, but the results show that the importance of history trajectory in this mode is relatively large, which may be related to the generally low speed during U-turns. The high importance of stopping and irregular road also verifies this conclusion, that is, deceleration or low speed will lead to a greater importance of history trajectory features.

Figure 8 shows the importance results of surrounding agents under different behavior modes. It can be seen that the importance of U-turn, go straight, irregular road sections, and stopping is relatively large, and the importance of lane change is the smallest. The reasons may be as follows: First, U-turn, go straight, and stopping are all carried out near intersections, involving vehicle interactions in multiple directions; second, in the Waymo dataset, irregular roads generally involve vehicle interactions. In addition, lane changes are generally carried out on the road section, and there are fewer vehicles involved in the interaction, so the corresponding feature importance is the smallest. The higher feature importance in the turn left and right cases also verifies our reason, that is, as the number of interacting agents increases, the importance of the corresponding neighboring agents will also increase.

Figure 9 shows the importance of maps under different be-

havior modes. It can be seen that the importance of maps is relatively large in the case of U-turns, turn right, turn left, and stopping, and the importance is the smallest in the case of irregular road. The reasons may be as follows: U-turns, turn right, turn left, and stopping are all carried out near intersections, and they need to follow the lane lines and cannot change lanes easily. Their driving decisions are closely related to maps. In addition, special roads generally have few traffic signals, so the corresponding features are the least important. Going straight and lane change are generally possible at intersections or road sections. When on the road section, the dotted line can change at will, and future decisions are less affected by the map, so the importance is in the middle.

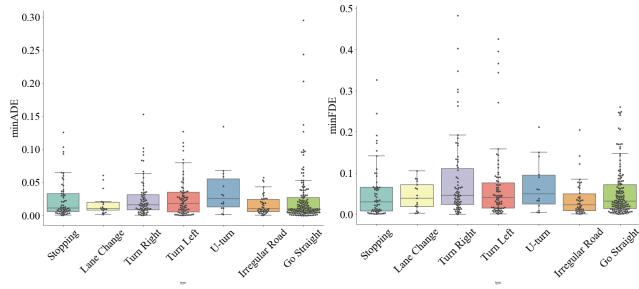


Figure 7: The results of the trajectory prediction error under different traffic rule compliance caused by history trajectory.

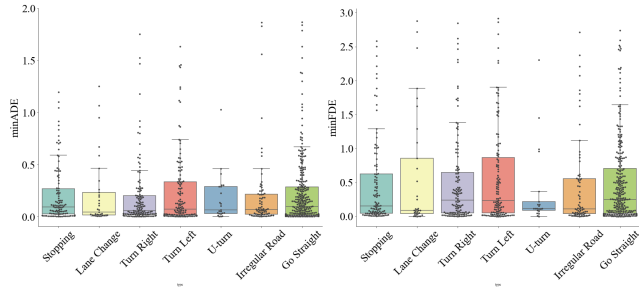


Figure 8: The results of the trajectory prediction error under different traffic rule compliance caused by neighboring agents.

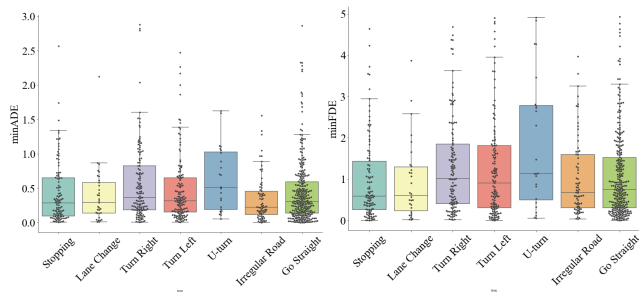


Figure 9: The results of the trajectory prediction error under different traffic rule compliance caused by map.